

Plasma Performance and Impurity Behavior in Long Pulse Discharges on LHD

Y.Nakamura, Y.Takeiri, R.Kumazawa, M.Osakabe, T.Seki, B.J.Peterson, K.Ida, H.Funaba, M.Yokoyama, N.Tamura, A.Komori, S.Morita, K.Sato, K.Narihara, S.Inagaki, T.Tokuzawa, S.Masuzaki, J.Miyazawa, N.Noda, T.Mutoh, T.Shimozuma, K.Kawahata, Y.Oka, H.Suzuki, N.Ohyabu, T.Akiyama¹, N.Ashikawa, M.Emoto, P.Goncharov², M.Goto, H.Idei, K.Ikeda, S.Imagawa, M.Isobe, O.Kaneko, H.Kawazome³, K.Khlopenkov, T.Kobuchi, A.Kostrioukov, S.Kubo, Y.Liang, T.Minami, T.Morisaki, S.Murakami, S.Muto, K.Nagaoka, Y.Nagayama, H.Nakanishi, Y.Narushima, K.Nishimura, T.Notake⁴, H.No zato⁵, S.Ohdachi, S.Okamura, T.Ozaki, A.Sagara, T.Saida², K.Saito, S.Sakakibara, R.Sakamoto, M.Sasao, M.Sato, M.Shoji, N.Takeuchi⁴, K.Tanaka, M.Y.Tanaka, K.Toi, Y.Torii⁴, K.Tsumori, K.Y.Watanabe, T.Watari, Y.Xu, H.Yamada, I.Yamada, S.Yamamoto⁴, T.Yamamoto⁴, S.Yoshimura, Y.Yoshimura, M.Yoshinuma, K.Itoh, T.Mito, K.Ohkubo, I.Otake, T.Satow, S.Sudo, T.Uda, K.Yamazaki, K.Matsuoka, O.Motojima, Y.Hamada, M.Fujiwara

National Institute for Fusion Science, 322-6 Oroshi-cho, Toki 509-5292, Japan

1) Research Laboratory for Nuclear Reactors, Tokyo Institute of Technology, Tokyo, Japan

2) Department of Fusion Science, School of Mathematical and Physical Science, Graduate University for Advanced Studies, Hayama, 240-0193, Japan

3) Graduate School of Energy Science, Kyoto University, Uji 611-0011, Japan

4) Department of Energy Engineering and Science, Nagoya University, 464-8603, Japan

5) Graduate School of Frontier Sciences, The University of Tokyo 113-0033, Japan

e-mail contact of main author: ynakamu@lhd.nifs.ac.jp

Abstract. The superconducting machine LHD has conducted long pulse experiments for four years to achieve long-duration plasmas with high performance. The operational regime was largely extended in the discharge duration and the plasma density. In this paper, the plasma characteristics, in particular, plasma performance and impurity behavior in long pulse discharges are described. Confinement studies show that global energy confinement times are compared with those in short-pulse discharges. Long sustainment of high performance plasma, which is equivalent to the previous achievement in other devices, was demonstrated. Long pulse discharges enabled us to investigate impurity behavior in a long time-scale. Intrinsic metallic impurity accumulation was observed in a narrow density window ($2 \sim 3 \times 10^{19} \text{m}^{-3}$) only for hydrogen discharges. Finally, impurity accumulation control with an externally induced magnetic island at the plasma edge was demonstrated.

1. Introduction

Demonstration of high confinement, long-duration discharges is one of the most challenging issues for magnetic fusion research. The achievement of this goal requires the development of heating scenarios (also current drive scenario for tokamaks) as well as solving particle and heat flux problems in steady state. Such investigations are particularly suited for the superconducting Large Helical Device (LHD) (major radius $R = 3.6 - 3.9$ m, minor radius $a = 0.6$ m, toroidal field on axis $B = 2.9$ T) research program which is aimed at the study of long-duration and high-performance plasmas [1]. LHD has a fully superconducting coil system [2], which generates a heliotron magnetic configuration ($l/m = 2/10$) in steady state for plasma confinement. Helical plasmas require no plasma current drive and can be sustained only by injecting the power for plasma heating. Therefore LHD could provide a new platform for fusion research on steady state operation with net current free plasmas. This device has an intrinsic helical divertor configuration and plasma experiments have been performed with the open divertor configuration so far [3]. The divertor target plates and the plasma vessel were designed and constructed so as to remove a steady state heat load of 3 MW [4, 5]. The heating systems (ECH, NBI and ICH) have been also developed to achieve an injection of 3MW total heating power in steady state [4]. The near future target is to demonstrate a steady state one-hour discharge with 3 MW heating. This paper summarizes the recent results on long pulse operation and its plasma characteristics obtained on LHD. After last IAEA conference, big

progresses have been made in discharge duration and operational density regime. The NBI heated plasma was sustained up to 110 s and a steady-state ICRF heated plasma with the discharge duration of 2 minutes was achieved. The next section reports on the progress towards steady state operation in LHD. Confinement properties of long-duration plasmas are discussed in section 3. Finally, impurity behavior and accumulation control in long pulse discharges are described in section 4.

2. Progress towards steady-state operation

Our efforts towards steady-state operation have been mainly devoted to the extension of discharge duration using both NBI and ICRF heating systems. The discharges obtained during the 1998-1999 experimental campaign are described in details in Refs. [4 - 6], including the historical description and the development of heating system. Before the 1999 campaign, all the strike points at the divertor legs were covered with graphite tiles, and it enabled us to enlarge the operational range of density and duration to a great extent. The divertor plates and the plasma vessel were cooled by water for the capability of steady-state operation with an injection power of 3 MW. However, the available power of heating systems (NBI, ICRF) was restricted for long pulse operation as shown in Fig. 1, where the discharge duration and the operational density are plotted for the injection power. In the NBI heating system, the limitation on the injection power was caused by the lost of stable operation of ion sources due to the temperature increase of plasma electrodes and the heat-up of molybdenum protecting plates at the injection port, which was not directly cooled by water. For NBI discharges, it was easy to raise the plasma density and a high-density discharge with a maximum density of $6.7 \times 10^{19} \text{m}^{-3}$ was sustained for 10 s with the power of 2 MW. ICRF long-pulse experiments with H-minority heating in helium plasmas have been made smooth progress in extending the discharge duration [7]. In fact, a two minute long-duration discharge in the 2001 campaign was achieved only after several long-pulse shots since the first trial for long pulse operation [8]. For ICH discharges, the injected radio frequency (rf) power from a pair of loop antennas was restricted by the electric break down and heat-up of rf amplifiers. The plasma density achieved with ICH remained at $1.15 \times 10^{19} \text{m}^{-3}$ even for high power operation (1.1 MW, 5 s). The maximum density is very low compared to that ($5.9 \times 10^{19} \text{m}^{-3}$) obtained with the corresponding NBI power. This density limit may be due to some reason different from the usual density limit [9], which is one of major concerns of ICH experiment in the coming experimental campaign.

Figure 2 shows the longest duration discharge with ICH ($P_{\text{ICH}} \sim 0.35 \text{ MW}$) alone. The helium plasma with minority hydrogen ions was sustained for 120 s with the density of around $0.8 \times 10^{19} \text{m}^{-3}$ and the electron temperature of 1.3 keV from ECE signals. The ion

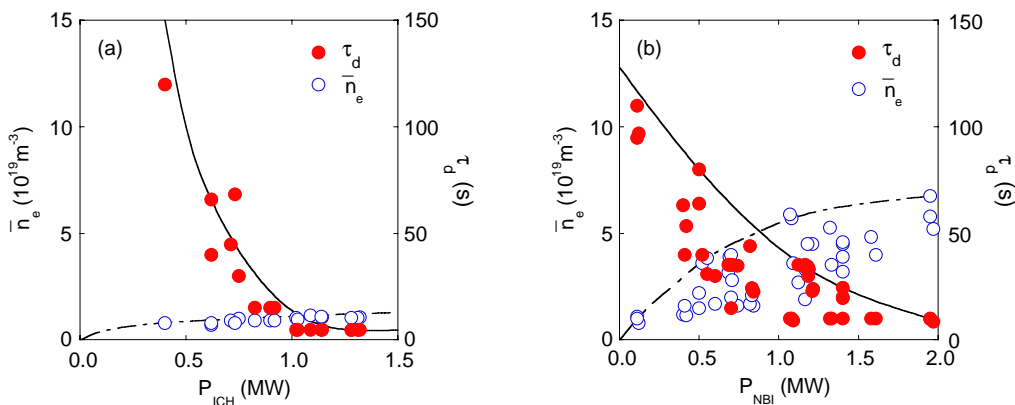


FIG. 1. Operational density and discharge duration for (a) ICRF and (b) NBI heated plasmas.

temperature was around 1.3 keV, which was measured from Doppler broadening of TiXXI (0.261 nm) using an x-ray crystal spectrometer. In this discharge, the amount of gas puffing was manually controlled by an operator watching a density signal from a far-infrared (FIR) interferometer. The radiation with a hollow profile [10] as well as the impurity line emissions (CIII, OV) was kept almost constant during the discharge. Spectroscopic and soft x-ray measurements show that there was no impurity accumulation of metal. The NBI heated plasma was also sustained for 110 s with a very low injection power of 0.11 MW. In spite of the low power level, the plasma with the density of $1.0 \times 10^{19} \text{m}^{-3}$ and the temperature of 0.35 keV was obtained by exceeding the radiation barrier. Demonstration of long-duration discharges with high performance is illustrated by Fig. 3 which shows plasma performance (through the usual criterion $n\tau_E T_{i0}$) versus pulse duration, and where the present results stand with respect to ITER objectives. The large tokamaks can produce a reactor-grade high performance plasma and a steady state plasma for more than 3 h was demonstrated in the small superconducting tokamak TRIAM [11, 12]. However, it is not enough to accumulate a database for long sustainment of high performance plasma required in ITER. In LHD, since the helical plasma requires no plasma current drive, various heating methods (ECH, NBI, ICH) can be applied for sustaining the plasma with each heating alone. First of all, the ECH plasma was sustained for 2 min with the input power of 50 kW [13]. The long pulse operation of high performance ECH plasma would require the development of steady-state high power gyrotron and transmission line. The NBI heated plasma was very stably sustained with high performance as well as in short-pulse discharges. The plasma performance in the 80 s discharge is superior to the previous achievement in Tore Supra [14]. One more neutral beam line, which is available for long pulse operation, has been installed and tested in the last experimental campaign. Further extension to high performance regime can be expected for NBI long pulse discharges. For ICH system, a new steady-state RF generator is now preparing for the next experimental campaign and the first goal is placed on steady state operation with 1 MW for more than 30 min.

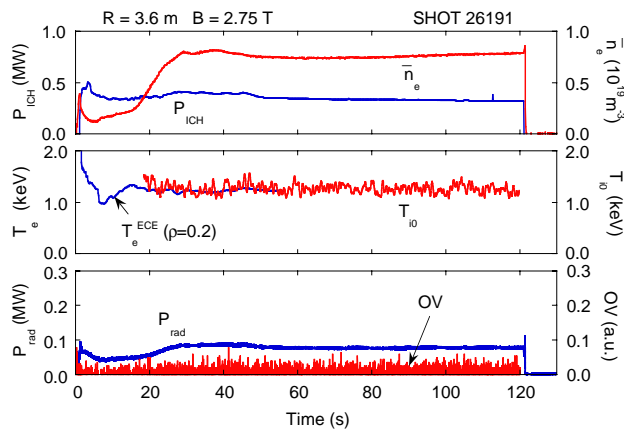


FIG. 2. Two minutes discharge with ICRF heating alone.

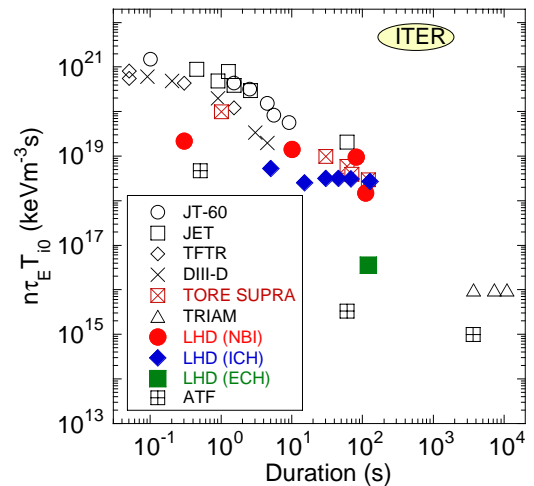


FIG. 3. Plasma performance vs pulse duration.

3. Plasma confinement characteristics of long pulse discharges

The energy confinement characteristics in LHD have been mainly investigated using short-pulse discharges with $\tau_d < 3$ s [15]. The LHD experiments in the inward shifted configuration ($R = 3.6$ m) indicated an improvement by a factor of 1.5 in τ_E (ISS95 scaling) without the confinement degradation due to MHD instabilities, which are predicted in an ideal MHD analysis. It is of great concern whether the improved LHD plasmas could be maintained

over a period of long time. Figure 4 shows a typical long pulse discharge with high performance. The target plasma was produced by ECH and the NBI power of around 1.5 MW was injected into the plasma for 10 s. The plasma density was controlled by hydrogen gas puffing, the amount of which was preprogrammed until 1 s and then controlled with a feedback loop so as to keep the density constant. As seen in Fig. 4, although the large amount of gas puffing was required for rising up the density, the gas puff rate was reduced with time. This suggests that the wall pumping is strong in the density build-up phase and the wall recycling increases with time as indicated by the recycling coefficient R [16]. The plasma temperature and density were kept constant and the profiles remained unchanged until the end of the discharge. The energy confinement time reaches up to 0.3 s and the enhancement factor in ISS95 scaling remains at around 1.4 during the discharge. There was no sign of confinement degradation in this discharge. It was evident that the high performance plasma obtained in short-pulse discharges can be sustained over a period of long time. However, the density scan revealed a new feature of long-duration plasma. Figure 5 shows the dependence of normalized plasma stored energy on the line averaged electron density. The open circles represent the plasmas in the initial stage of the discharge ($t = 2 \sim 3$ s) and the solid ones the plasmas at the end of the discharge ($t = 8 \sim 10$ s). A scaling of the normalized stored energy can be derived from the ISS95 scaling: $W_p / P_{\text{dep}}^{0.41} = 0.11 \bar{n}_e^{0.51}$ where P_{dep} is the NBI deposition power calculated by using a shine-through power, which was measured with calorimeter arrays embedded in beam facing armor plates [17]. The plasmas at the initial stage showed the ISS95 scaling with an enhancement factor of 1.4. On the other hand, a significant decrease of the store energy was observed after about 10 s in the density range of $2 \sim 4 \times 10^{19} \text{ m}^{-3}$. When the density was kept constant in this

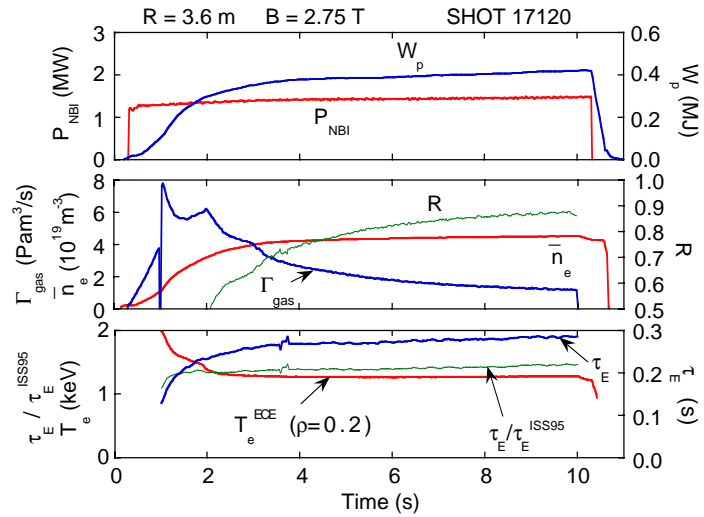


FIG. 4. A typical long pulse discharge with high performance. The enhancement factor ($\tau_E / \tau_E^{\text{ISS95}}$) is maintained at around 1.4.

The plasma temperature and density were kept constant and the profiles remained unchanged until the end of the discharge. The energy confinement time reaches up to 0.3 s and the enhancement factor in ISS95 scaling remains at around 1.4 during the discharge. There was no sign of confinement degradation in this discharge. It was evident that the high performance plasma obtained in short-pulse discharges can be sustained over a period of long time. However, the density scan revealed a new feature of long-duration plasma. Figure 5 shows the dependence of normalized plasma stored energy on the line averaged electron density. The open circles represent the plasmas in the initial stage of the discharge ($t = 2 \sim 3$ s) and the solid ones the plasmas at the end of the discharge ($t = 8 \sim 10$ s). A scaling of the normalized stored energy can be derived from the ISS95 scaling: $W_p / P_{\text{dep}}^{0.41} = 0.11 \bar{n}_e^{0.51}$ where P_{dep} is the NBI deposition power calculated by using a shine-through power, which was measured with calorimeter arrays embedded in beam facing armor plates [17]. The plasmas at the initial stage showed the ISS95 scaling with an enhancement factor of 1.4. On the other hand, a significant decrease of the store energy was observed after about 10 s in the density range of $2 \sim 4 \times 10^{19} \text{ m}^{-3}$. When the density was kept constant in this

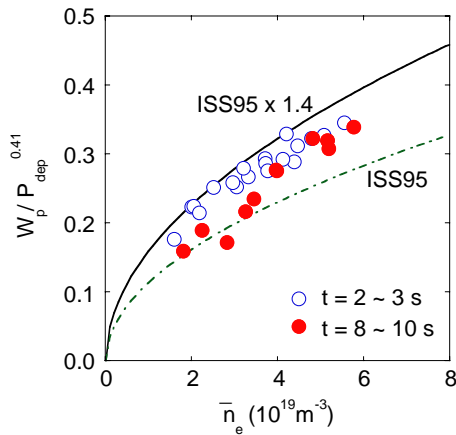


FIG. 5. Dependence of normalized stored energy on line-averaged electron density. The stored energy is normalized by the deposition power with the ISS95 scaling.

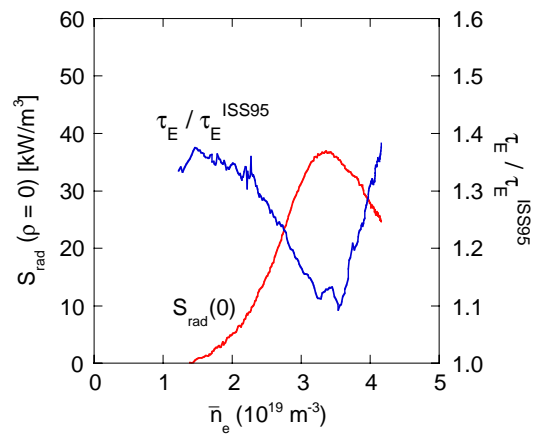


FIG. 6. Correlation between central radiation and the enhancement factor in τ_E . Each line indicates the time trace during the discharge (shot 17093).

region, the plasma performance was remarkably degraded with time and the stored energy decreased up to 68 % at the end of the discharge ($t = 10$ s). This degradation of plasma performance may be related to the energy loss caused by the radiation due to metallic impurity accumulation, which will be described in Sec. 4. Figure 6 shows a relationship between the enhancement factor in τ_E and the radiation emissivity at the plasma center in the density ramp-up discharge (shot 17093). When the density increased with time, the central radiated power increased remarkably with increasing the density, thereby leading to the reduction of enhancement factor. In the high-density region, the central radiated power decreased and the plasma performance was recovered rapidly with the decrease of the radiation. Since the radiated power density corresponds to about 32 % of the deposited power density in the core region, the power balance of core plasma may be largely affected by the strong core radiation. On the contrary, long-pulse operation for more than 10 s has been carried out with helium gas puffing and there was no sign of impurity accumulation. Therefore, no plasma confinement degradation has been seen in all operational regime. Both NBI and ICRF heated long-duration plasmas indicated an enhancement factor of around 1.5 relative to the ISS95 scaling in the inward shifted configuration ($R = 3.6$ m) as well as in short-pulse discharges.

4. Impurity behavior in long pulse discharges

4.1 Long time-scale impurity accumulation

In a variety of long pulse discharges, we found that metallic impurity accumulation was observed only in NBI heated hydrogen discharges in a narrow density window of $2 \sim 3 \times 10^{19} \text{ m}^{-3}$ [18]. Figure 7 shows a typical long pulse discharge with impurity accumulation. The plasma was initiated by ECH and heated with a neutral beam line with the injection power of 1.1 MW. The plasma density was controlled by hydrogen gas puffing with a feedback loop and kept to be $2.9 \times 10^{19} \text{ m}^{-3}$ until 28 s. A remarkable increase of central radiation ($\rho = 0$) is

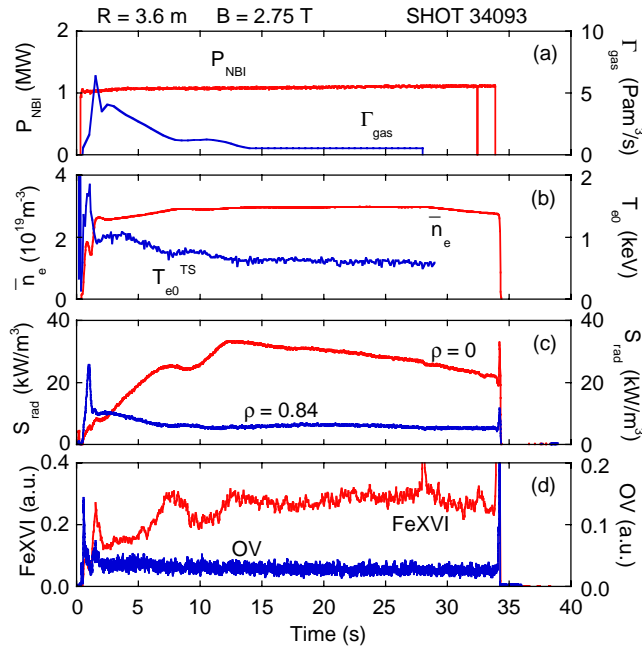


FIG. 7. A typical NBI hydrogen discharge with long time-scale impurity accumulation. The plasma density is kept constant by a gas puff system with a feedback loop.

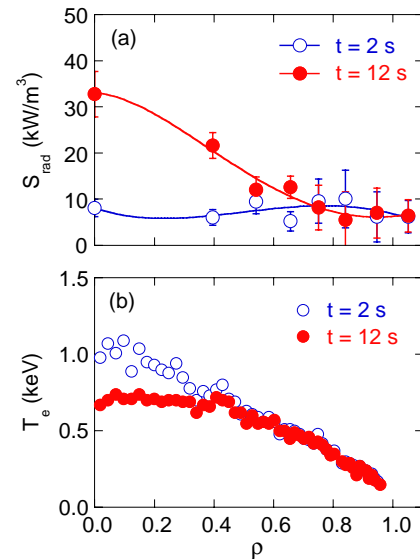


FIG. 8. Temporal variation of (a) radiation and (b) electron temperature profiles. The radiation profile is strongly peaked at 12 s and then the temperature profile becomes flat in the core region.

observed in a long time-scale until 12 s and the radiation decreases very slowly with time. On the other hand, the radiation at the peripheral region ($\rho = 0.84$) decreases gradually until 10 s and then remains almost constant. Clear evidence of impurity accumulation is observed in the profiles of radiated power density as shown in Fig. 8(a). A strong core radiation is observed at 12 s and then the radiation profile is maintained until the end of the discharge. This increase of central radiation causes a significant decrease of central electron temperature as shown in Fig. 8(b). However, there is no radiation collapse in these discharges. The core density profile is flat in the initial stage and it becomes slightly peaked with impurity accumulation. The low-Z impurity emission (OV) originating from the edge plasma is kept constant during the discharge (Fig. 7(d)). On the other hand, the time evolution of heavy metallic impurity emission (FeXVI), which reflects the impurity behavior in the core region, is similar to that of the central radiation. Spectroscopic and soft x-ray measurements indicated that the main metallic impurity was iron, which is an element of the plasma wall material.

The density scan during the long-duration discharge revealed a dramatic change of impurity behavior. In the density ramp-up discharge, the central radiation increases with the density and then turns down in high-density region. Such a remarkable change of impurity behavior was also observed in constant density discharges. Figure 9 shows the time evolution of central radiated power density and the most prominent metallic emission (FeXXIII), which originates from the core plasma ($T_{e0} > 1$ keV), for the discharges with different plasma densities. Remarkable temporal increases of the central radiation and the iron line emission were found only for the discharge with $2.7 \times 10^{19} \text{m}^{-3}$. This implies that there is an impurity accumulation window in the operational regime. Figure 10 shows the classification of long-duration plasmas on n - T space from the point view of impurity behavior. The discharges with impurity accumulation (crosses) were distinguished from those without accumulation and with pump-out (open squares and solid circles). The solid line represents the transition between the plateau regime and the Pfirsch-Schlüter regime for iron impurity. The broken line represents the transition between the electron root and the ion root for background plasma in nonaxisymmetric torus. This indicates a critical point of the specific space where the plasma has multiple solutions for the ambipolar electric field [19]. In the region of high-temperature and low-density (low collisionality), metallic impurities do not accumulate in the plasma core due to the positive radial electric field in electron root. Radial electric field measurements with CXRS show that the transition from positive electric field to negative one occurs at the plasma parameter space with the density $1 \times 10^{19} \text{m}^{-3}$ and the temperature 2 keV. In fact, small positive electric fields were observed even in the density range of ion root near the transition to electron root [20]. In the region of low-temperature and high-density (high collisionality),

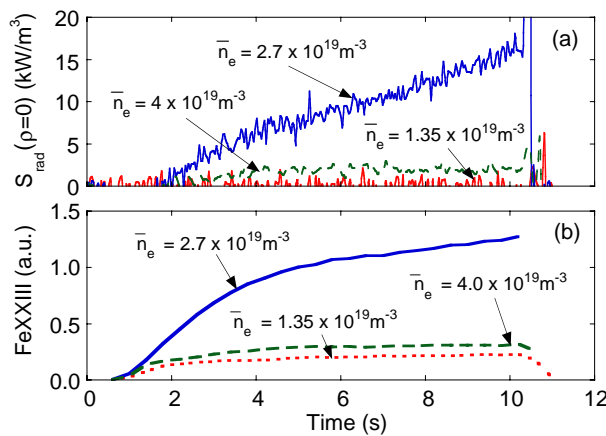


FIG. 9. Time evolution of (a) central radiation and (b) FeXXIII emission for the discharge with constant densities. Remarkable increases are observed only for the discharge with $2.7 \times 10^{19} \text{m}^{-3}$.

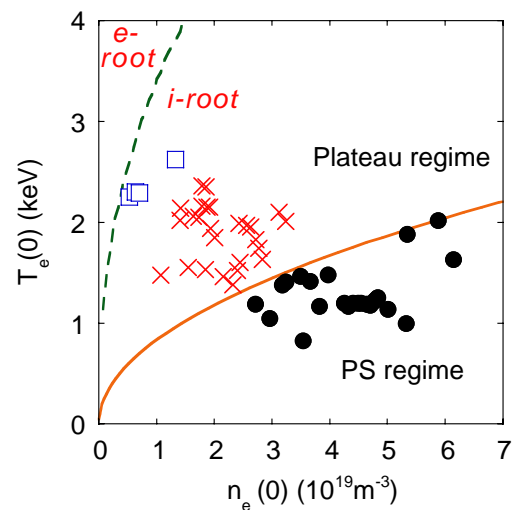


FIG. 10. A n - T diagram for impurity behavior in long pulse discharges. The crosses indicate the plasma with impurity accumulation.

there is no sign of impurity accumulation, which may be caused by the dominant contribution of temperature gradient in the PS regime (“temperature screening effect”). In the intermediate region, which corresponds to the plateau regime for impurity ions, impurity accumulation is always observed with a long time constant (~ 10 s). In our helical device, it is found that there is a narrow window for impurity accumulation in the plasma parameter space (collisionality space). Impurity pellet injection experiments show that the decay time of the impurity line emission increases with increasing the density and the experimental results are in qualitative agreement with the impurity behavior in long pulse experiments [21]. On the whole, the qualitative features are consistent with neoclassical impurity transport [18]. However, the negative impurity flux (accumulation) is not found in a simple analysis with neoclassical theory, which includes the expression for axisymmetric torus plasmas. The detailed analysis with a complete set of impurity transport theory for nonaxisymmetric plasmas would be required for understanding the physical mechanism underlying the impurity behavior in long pulse discharges.

4.2 Impurity accumulation control

In order to realize a steady state operation with high performance plasma, it is of great importance to reduce impurity concentration or prevent impurities from penetrating into the core plasma. In the previous LHD experiments [22], the influence of magnetic islands on impurity behavior was observed by using external perturbation coils, which produce a $n/m = 1/1$ magnetic island at the plasma edge. Therefore, impurity accumulation control with the magnetic islands was attempted in long pulse discharges as shown in Fig. 11, where both discharges with and without the magnetic island are indicated. The perturbation field is applied at 10 s and increased linearly until 28 s. A drastic change of impurity behavior was observed at 3 s after the application of perturbation field. The central radiation decreases on a large scale and a significant increase of the central electron temperature is observed. At that time, both magnetic islands inside and outside of the torus appear clearly with the size of

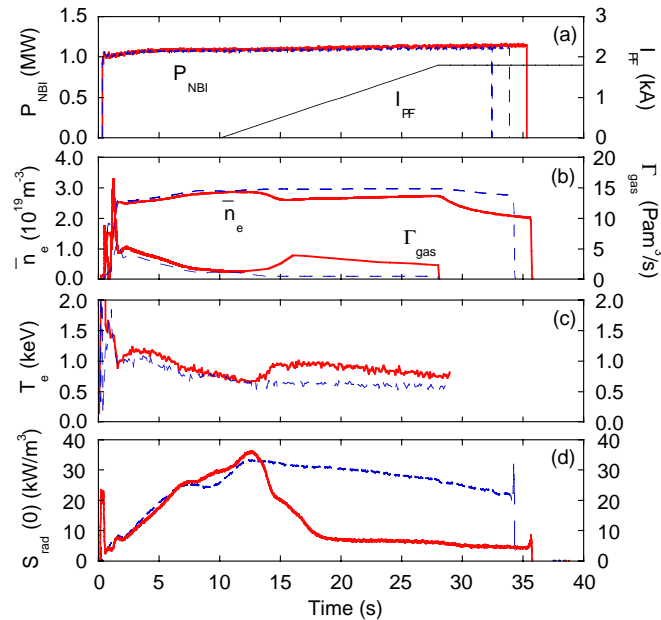


FIG. 11. Impurity accumulation control by the application of perturbation field. A magnetic island is produced by the perturbation coil current (I_{PF}). The solid and broken lines indicate the discharges with and without magnetic island, respectively.

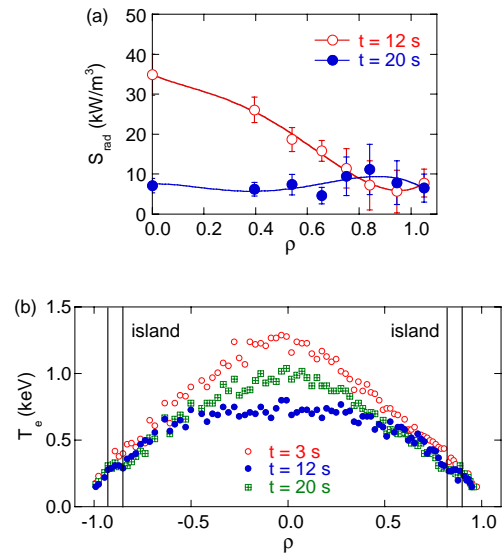


FIG. 12. Temporal variation of (a) radiation and (b) electron temperature profiles for the discharge with magnetic island. The strong core radiation disappears by the application of perturbation field.

around 7 cm as seen in the temperature profile (Fig. 12(b)). The peaked radiation profile returns to the hollow one by applying the perturbation field (Fig. 12(a)) and the impurities in the core plasma may diffuse out by the reduction of impurity influx. Another important feature in this discharge is the change of particle transport caused by the application of perturbation field. As seen in Fig. 11(b), a large difference of gas puffing rate between with and without the magnetic island is observed and the gas fueling rate is very low for the discharge with impurity pump-out by means of magnetic island formation. This method of impurity accumulation control with the magnetic island could be applied for long pulse operation in future.

5. Conclusions

Big progresses towards long pulse operation have been made in LHD experiments for four years. Long pulse operation with high plasma performance has been demonstrated with both NBI and ICRF heating. In particular, the achievement of two minutes discharge with ICH alone enabled us to open a new regime in high confinement and long-duration discharges. Confinement characteristics of long-duration plasmas were completely similar to those in short-pulse discharges. The improved confinement plasmas in the inward shifted configuration were sustained over a period of long time for both NBI and ICRF discharges. Long pulse experiments showed impurity accumulation in a long time-scale (~ 10 s) only for NBI heated hydrogen discharges. The intrinsic metallic impurities (mainly iron) were accumulated in a specific range of the operational plasma density ($2 \sim 3 \times 10^{19} \text{m}^{-3}$), that is, a narrow collisionality regime of the core plasma. The successful control of impurity accumulation was demonstrated with a magnetic island ($n/m = 1/1$) at the plasma edge in long pulse discharges.

References

- [1] IYOSHII, A., et al., Nucl. Fusion **39** (1999)1245.
- [2] MOTOJIMA, O., et al., Nucl. Fusion **40** (2000)599.
- [3] FUJIWARA, M., et al., Nucl. Fusion **41** (2001) 1355.
- [4] FUJIWARA, M., et al., Nucl. Fusion **40** (2000) 1157.
- [5] NODA, N., et al., Nucl. Fusion **41** (2001) 779.
- [6] TAKEIRI, Y., et al., Plasma Phys. Control. Fusion **42** (2000) 147.
- [7] KUMAZAWA, R., et al., Phys. Plasmas **8** (2001) 2139.
- [8] SEKI, T., et al., Proc. of 14th Topical Conf. on Radio Frequency Power in Plasmas, Oxnard, California, May 2001, CP595, p. 67.
- [9] SUDO, S., et al., Nucl. Fusion **30** (1990) 11.
- [10] PETERSON, B. J., et al., J. Nucl. Mater. **290-293** (2001) 930.
- [11] ITOH, S., et al., Nucl. Fusion **39** (1999) 1257.
- [12] SAKAMOTO, M., et al., IAEA-CN-94/EX/P4-07, this conference.
- [13] SHIMOZUMA, T., et al., Fusion Eng. Des. **53** (2001) 525.
- [14] EQUIPE TORE SUPRA (presented by B. Saoutic), Fusion Energy 1996 (Proc. 16th Int. Conf. Montreal, Canada 1996), IAEA, Vol. 1, Vienna (1997) 141.
- [15] YAMADA, H., et al., Nucl. Fusion **41** (2001) 901.
- [16] NAKAMURA, Y., et al., J. Nucl. Mater. **290-293** (2001) 1040.
- [17] OSAKABE, M., et al., Rev. Sci. Instrum. **72** (2001) 590.
- [18] NAKAMURA, Y., et al., Plasma Phys. Controlled Fusion **44** (2002) 2121.
- [19] YOKOYAMA, M., et al., Nucl. Fusion **42** (2002) 143.
- [20] IDA, K., et al., Phys. Rev. Lett. **86** (2001) 5297.
- [21] TAMURA, N., et al., Proc. of 29th EPS Conf. on Plasma Phys. And Contr. Fusion, Montreux, June 2002, ECA Vol. 28B, P-1.126.
- [22] KOMORI, A., et al., Phys. Plasmas **8** (2001) 2002.